Evolution of the Liouville density of a chaotic system

Asher Peres* and Daniel Terno
Department of Physics, Technion–Israel Institute of Technology, 32 000 Haifa, Israel
(Received 30 May 1995)

An area-preserving map of the unit sphere, consisting of alternating twists and turns, is mostly chaotic. A Liouville density on that sphere is specified by means of its expansion into spherical harmonics. That expansion initially necessitates only a finite number of basis functions. As the dynamical mapping proceeds, it is found that the number of non-negligible coefficients increases exponentially with the number of steps. This is in contrast to the behavior of a Schrödinger wave function, which requires, for the analogous quantum system, a basis of fixed size.

PACS number(s): 05.45.+b

I. INTRODUCTION

Chaos is commonly associated with nonlinear dynamics, and the elusiveness of quantum chaos is sometimes attributed to the fact that Schrödinger's equation is linear. However, the different behaviors of classical and quantum systems cannot be explained so simply. Any classical Hamiltonian motion can be described by means of a (possibly singular) Liouville density, and the evolution of the latter obeys a linear equation, which can be written as

$$i\,\partial f/\partial t = Lf. \tag{1}$$

Here f is a function of the q^n and p_n, which are independent variables parametrizing phase space, and L is the Liouville operator, or Liouvillian,

$$L = \sum_n \left(\frac{\partial H}{\partial p_n}\right)\left(-i\,\frac{\partial}{\partial q^n}\right) - \left(\frac{\partial H}{\partial q^n}\right)\left(-i\,\frac{\partial}{\partial p_n}\right). \tag{2}$$

This operator is formally "Hermitian" (over a suitable domain of Liouville functions f) so that the time evolution of f is a *unitary mapping* of phase space. Namely, if there is another Liouville function g, which also satisfies Eq. (2), the scalar product $\int f^* g \prod dq^n dp_n$ is invariant in time. This is Koopman's theorem [1].

The essential difference between the Liouville equation and the Schrödinger equation is that, in the generic nonintegrable case, the Liouvillian has a continuous spectrum, in which an infinite number of discrete lines may be embedded [2]. Let U be the unitary operator that generates the time evolution of the Liouville density. If the dynamical system has a finite measure, U has at least one eigenvalue equal to 1, corresponding to equilibrium. Moreover, it can be proved [2] that, if the system is ergodic, but not mixing, that eigenvalue is nondegenerate and all the other eigenvalues of U form a subgroup of the circle group. On the other hand, for a mixing system, which also has a single nondegenerate eigenvalue 1, the rest of the spectrum is absolutely continuous. A generic dynamical system may have some regions of phase space that are subject to mixing, others that are only ergodic, and still others that are not even ergodic. Such a system is called "decomposable" [3]. In that case, the spectrum of U is continuous, with an infinite number of discrete lines embedded in it. In particular, the eigenvalue 1, and possibly others, are degenerate.

These properties give rise to fundamental differences between the evolution of Liouville densities and that of quantum wave functions for bounded systems that have discrete spectra in quantum theory. In particular, any quantum state can always be represented, with arbitrary accuracy, by a *finite* number of energy eigenstates. The time evolution of a bounded quantum system therefore is multiply periodic and will sooner or later have recurrences [4]. On the other hand, since the Liouville equation involves a continuous spectrum, the evolution of a generic Liouville density cannot be represented by a finite number of terms. Thanks to this property, a Liouville density is able to become more and more convoluted with the passage of time and it may form intricate shapes with exceedingly thin and long protuberances, something that a quantum wave function cannot do with a conventional Hamiltonian [5].

The purpose of this work is to apply to the Liouville equation some of the mathematical techniques that are standard in quantum mechanics. The Liouville density f is expanded into a complete set of orthonormal functions

$$f(q,p) = \sum_n c_n\, u_n(q,p). \tag{3}$$

(Note that these u_n are not eigenfunctions of the Liouvillian: the latter do not form a complete set, since part of the spectrum is continuous.) The Liouville equation (1) becomes

$$i\,dc_m/dt = \sum_n L_{mn}\, c_n, \tag{4}$$

where L_{mn} is a Hermitian matrix of infinite order. It

*Electronic address: peres@photon.technion.ac.il

1063-651X/96/53(1)/284(7)/$06.00

follows that $\sum |c_n|^2$ is constant in time. However, even if we start with a small number of nonvanishing c_n, it turns out, as will be seen below, that as time passes, f spreads over more and more u_n. A convenient quantitative measure of this spread is the entropylike expression [6]

$$S = -\sum_n |c_n|^2 \ln|c_n|^2. \tag{5}$$

The intuitive meaning of S is that e^S is a rough indication of the number of basis vectors that are appreciably involved in the expansion of f in Eq. (3). An appropriate name for S could be "dimensional entropy" (or D entropy). Another, roughly equivalent expression is the "inverse participation factor" [7], namely, $1/\sum |c_n|^4$.

Since chaotic systems are characterized by the exponential divergence of neighboring trajectories, we expect that the number of basis functions needed for representing f (with a given level of accuracy) should also increase exponentially with time. In other words, we expect S to increase linearly with time for chaotic systems (in the asymptotic limit of large t). On the other hand, for regular systems, whose trajectories diverge linearly, we expect an asymptotically logarithmic growth of S. Of course, these are no more than qualitative expectations. The actual growth laws have to be found by explicit calculations.

In the following sections we shall investigate a simple dynamical model that has a well documented chaotic behavior, and it will be seen that these guesses are qualitatively correct. That model involves a discrete time variable, rather than a continuous time, in order to make calculations simpler. Instead of the continuous time evolution (4), there is a unitary transformation of the components c_n (explicitly given below).

II. THE TWIST AND TURN MAP

Consider a sequence of mappings of the unit sphere $x^2 + y^2 + z^2 = 1$, in which each step consists of a *twist* by an angle a around the z axis (namely, every xy plane turns by an angle az), followed by a 90° rigid *rotation* around the y axis. The result of these consecutive twist and turn operations is

$$\begin{aligned} x' &= z, \\ y' &= x \sin(az) + y \cos(az), \\ z' &= -x \cos(az) + y \sin(az). \end{aligned} \tag{6}$$

This map is obviously area preserving. It was extensively investigated, both classically and in quantum mechanics, by Haake, Kuś, and Scharf [8], who called it a "kicked top." (It is not really like the motion of a rigid top because of the torsion.) For low values of a, most classical orbits are regular (that is, they are quasiperiodic). As a increases, so does the fraction of chaotic orbits, until for $a = 3$ most of the sphere is visited by a single chaotic orbit, as may be seen in Fig. 1. That figure also shows the presence of "forbidden" areas, corresponding to regular regions located around fixed points of the map [9, 10]. All the following calculations refer to the case $a = 3$, unless stated otherwise.

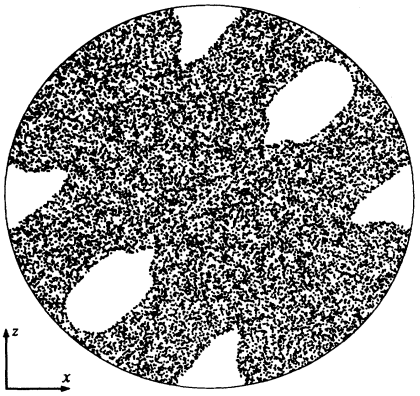

FIG. 1. Area-preserving projection of the hemisphere $y > 0$. The figure shows 20 000 points belonging to a single chaotic orbit. The empty regions are filled by regular orbits, not shown here.

The map (6) has interesting symmetries. Given any closed orbit, another closed orbit can be obtained by changing the signs of both x and z. This symmetry will be called R_y (it is a rotation by 180° around the y axis). Moreover, for any pair of distinct orbits related by R_y, it is possible to obtain a third orbit (of twice the length) by means of a 180° rotation of that pair of orbits around the x axis. These symmetries have important consequences for the classification of Liouville densities, as will be seen in Sec. III.

A characteristic property of each orbit is its Lyapunov exponent. In the present case, it may be defined as follows. Consider an infinitesimal circle drawn on the sphere around the initial point of a fiducial orbit. As the map proceeds, this infinitesimal circle is deformed into an infinitesimal ellipse, having the same area. The ellipse rotates and stretches or contracts in an "erratic" way at each step. Let a_n be the length of its semimajor axis after n steps. The Lyapunov exponent (per step) is defined as

$$\lambda = \lim_{n\to\infty} \frac{\ln(a_n/a_0)}{n}. \tag{7}$$

Such a limit indeed exists for a generic chaotic orbit [11, 12]. In the special case of a regular orbit, the pulsations of the ellipse are bounded and therefore $\lambda = 0$.

We have computed in this way the Lyapunov exponents for 10^5 orbits with randomly chosen initial points. Each orbit was terminated after 10^4 steps (this usually happened when the orbit was regular) or, for chaotic orbits, when the major axis of the ellipse exceeded 10^{16} (because of the inevitable loss of precision in any further computation). The details of the calculations are given in Appendix A and the results are displayed in Fig. 2. About 14% of the orbits are regular. For the chaotic ones, we obtained an average value (the uncertainty is one standard deviation):

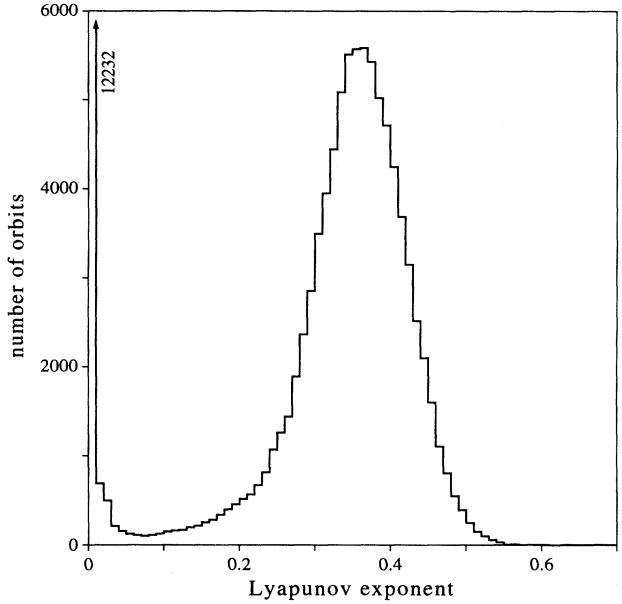

FIG. 2. Distribution of Lyapunov exponents for 10^5 randomly chosen orbits. Each bin of the histogram has width 10^{-2}.

$$\lambda = 0.346 \pm 0.071. \tag{8}$$

The dispersion in λ is a numerical artifact, also explained in Appendix A. Ideally, λ should have had a sharp value, the same for all chaotic open orbits. This dispersion free value can in principle be found by more sophisticated methods [13], allowing one to follow an orbit for many more steps. However, this was not needed for our purpose: the only reason that prompted us to actually evaluate the Lyapunov exponents for many different orbits was that we found widely different D entropies for different symmetry classes (see Fig. 4 below). We therefore checked the possible existence of two different categories of chaotic orbits. These would have been revealed by two separate chaotic peaks in Fig. 2 (besides the regular peak for $\lambda = 0$). As we see no indication of such a double peak, we can definitely rule out such a possibility, which was quite unlikely anyway.

III. MAPPING OF LIOUVILLE DENSITIES

Instead of considering individual orbits, that is, mapping of points into points, a more general approach, which gives instructive insights, is the mapping of Liouville densities. Let us imagine that an infinitesimal "mass" $\rho\, dA$ (which may be positive or negative) is attached to each area dA. Let us further assume that this mass is conserved during the twists and turns of the unit sphere, so that its density ρ obeys the linear law

$$\rho'(x', y', z') = \rho(x, y, z), \tag{9}$$

by virtue of $dA' = dA$. The mass density ρ thus behaves as an incompressible fluid or as a Liouville density. We shall henceforth call it by the latter name because Eq. (6) can be considered as a *canonical mapping*, for which the phase space is the unit sphere.

For the twist and turn map (6), these Liouville densities may belong to three invariant symmetry classes, according to their behavior under R_y and R_x (namely, 180° rotations around the y and x axes, respectively). For example, if $\rho = F(x^2, y^2, z^2, xyz)$ is a single valued function of its four arguments, this ρ is even under R_y and R_x and is mapped by Eq. (9) onto another function of the same type. Likewise, any $\rho = yF(x^2, y^2, z^2, xyz)$ is even under R_y and odd under R_x and is mapped by (9) onto a function of the same type. For instance, the function $\rho = y$ has this property because

$$\begin{aligned} y \to y' &= x\, \sin(az) + y\, \cos(az) \\ &= y \left[\cos(az) + \frac{xyz}{y^2} \frac{\sin(az)}{z} \right]. \end{aligned} \tag{10}$$

In general, any $\rho(x, y, z)$ can be written as the sum of three terms, belonging to one of the symmetry classes listed in Table I.

A natural way of expanding Liouville functions on the unit sphere is the use of spherical harmonics

$$\rho(\theta, \phi) = \sum_{l,m} C_{lm}\, Y_l^m(\theta, \phi), \tag{11}$$

where the angles θ and ϕ are related to the Cartesian coordinates in Eq. (6) in the usual way: $x = \sin\theta\, \cos\phi$, etc.

We shall use the common (but not universal) sign conventions [14, 15]

$$\begin{aligned} Y_l^m(\theta, \phi) &= \left[\frac{2l+1}{4\pi} \frac{(l-m)!}{(l+m)!} \right]^{1/2} (-1)^m\, e^{im\phi}\, P_l^m(\cos\theta), \\ Y_l^{-m}(\theta, \phi) &= (-1)^m\, Y_l^{m*}(\theta, \phi), \end{aligned} \tag{12}$$

where $m \geq 0$ and $P_l^m(\cos\theta)$ are the associated Legendre polynomials. The $Y_l^m(\theta, \phi)$ are othonormal, so that

$$C_{lm} = \int Y_l^{m*}(\theta, \phi)\, \rho(\theta, \phi)\, d\Omega, \tag{13}$$

where $d\Omega = \sin\theta\, d\theta\, d\phi$. In particular, the total mass, namely, $\int \rho d\Omega = \sqrt{4\pi} C_{00}$, is constant for our area-preserving map. We shall henceforth ignore the trivial C_{00} component and consider only the entropy of the other

TABLE I. Symmetry classes of Liouville functions.

R_y	R_x	Functional form
even	even	$\rho = F(x^2, y^2, z^2, xyz)$
even	odd	$\rho = yF(x^2, y^2, z^2, xyz)$
odd		$xF_1(x^2, y^2, z^2, xyz) + zF_2(x^2, y^2, z^2, xyz)$

ones.

The nontrivial C_{lm} transform as follows: during a twist, θ is constant, and

$$\phi \to \phi' = \phi + a\cos\theta. \tag{14}$$

We thus have $\rho'(\theta, \phi + a\cos\theta) = \rho(\theta, \phi)$, or

$$\rho'(\theta, \phi) = \rho(\theta, \phi - a\cos\theta), \tag{15}$$

whence

$$C'_{jm} = \int Y_j^{m*}(\theta, \phi)\, \rho(\theta, \phi - a\cos\theta)\, d\Omega, \tag{16}$$

because $d\Omega' = d\Omega$. Substitution of (11) into (16) then gives

$$C'_{jm} = \sum_l U_{jl}^{(m)}\, C_{lm}, \tag{17}$$

where the $U_{jl}^{(m)}$ are components of a unitary matrix

$$U_{jl}^{(m)} = \int Y_j^{m*}(\theta, \phi)\, Y_l^m(\theta, \phi)\, e^{-ima\cos\theta}\, d\Omega. \tag{18}$$

An accurate method for computing $U_{jl}^{(m)}$ for large j and l is described in Appendix B.

We thus see that a twist leaves m invariant, but it introduces all the $l \geq |m|$ (with exponentially small coefficients for large l), while a rotation mixes different m but leaves l invariant [16, 17]. This emergence of higher and higher l occurs only in the *classical* twist and turn map, which thus behaves in a quite different way from the corresponding quantum map [8, 9]. This is because in quantum theory l has the meaning of total angular momentum and the latter is a constant of the motion under a twist (which is generated by J_z^2), while the classical l has no such dynamical meaning and therefore need not be conserved.

Note that a pure twist is a regular motion: all the orbits are closed circles around the z axis. We examined the growth of S, as a function of a continuous twist angle a, for two maps starting with ρ proportional to x (odd symmetry class) or to y (even-odd symmetry). These are represented by initial states with

$$C_{11} = \mp C_{1,-1} = 1/\sqrt{2}, \tag{19}$$

respectively, and all other $C_{lm} = 0$. Since different values of m do not mix during a twist, the D entropy is the same in both cases. Figure 3 shows the result: the growth of e^S is roughly linear, as expected. The slope, however, appears to slowly decrease as the twist angle becomes larger.

We now turn our attention to the rotations of the unit sphere. With spherical harmonics used as a basis, the matrix representation of a 90° rotation is well known [16, 17]: the index l is not affected, and for each l the $(2l+1)$ components indexed by m undergo a unitary transformation. Appendix C explains how to construct accurately these unitary matrices (we proceeded up to $l = 500$).

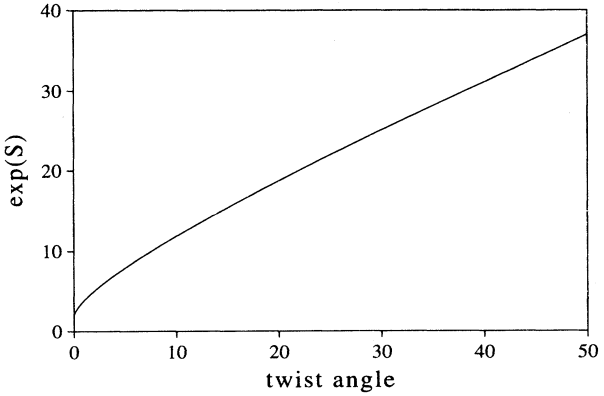

FIG. 3. Growth of the D entropy for a continuous twist, as a function of the twist angle.

We checked the accuracy of our numerical calculations by verifying that unitarity held at each step, with an error less than 10^{-8}. To achieve this result, we had to use a range of values of l that increased by a factor ~3.4 at each step. We thus had, at the fifth step, components C_{lm} with l up to 500. This implied that the rotation matrices had all possible odd orders up to 1001 and twist matrices had all orders up to 500. The next step would have exceeded the capacity of our computer (or entailed a severe loss of accuracy).

Figure 4 shows how S grows with the number of steps. In the case $a = 3$, we considered two different initial Liouville densities, given by Eq. (19). These functions, which belong to different symmetry classes, appear to have roughly linear rates of growth of their D entropies,

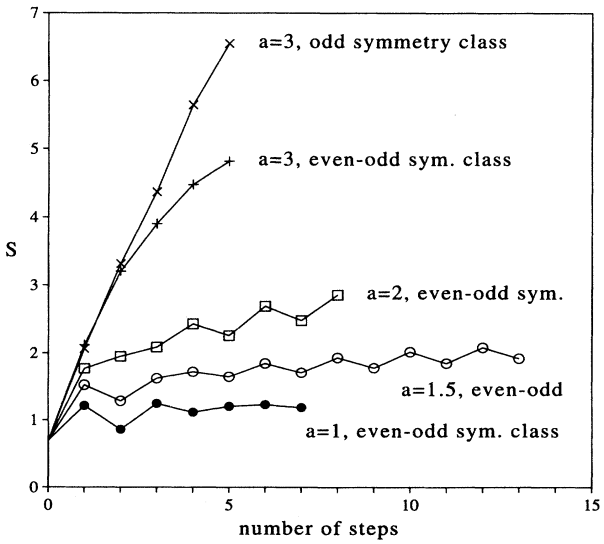

FIG. 4. Growth of the D entropy for the twist and turn map, for various values of the twist parameter a.

as expected (with a small negative second derivative, as in Fig. 3). Here the surprise is that these rates are manifestly different from each other. We must therefore conclude that the growth of the D entropy, contrary to the Kolmogorov-Sinai entropy [11, 12], is not related in a simple way to the Lyapunov exponents of individual orbits because generic aperiodic orbits have no symmetry.

We also performed similar calculations for some lower values of a. For $a = 2$, the twist and turn map is mostly regular, but there still are small chaotic regions [8]. These chaotic regions become almost invisible for $a = 1.5$ or less. As Fig. 4 shows, for these low values of a the growth of S is not uniform. Rather, S oscillates about a slowly increasing average. The reason is that, as the chaotic regions shrink, the projection of ρ over the discrete part of the spectrum becomes more important. If only a few eigenvectors are appreciably involved, their contribution to ρ is almost periodic, and this results in an oscillatory behavior of the D entropy.

We also found oscillations for $a = 3$, when we started with an unsymmetrized f, for example, with $C_{11} = 1$ and all other $C_{lm} = 0$. These oscillations, however, are of a completely different nature. They are caused by ordinary interference between components of ρ belonging to different symmetry classes and are similar to the familiar "collapse and revival" phenomena reported in Ref. [8].

IV. CONCLUDING REMARKS

We found some results that were not unexpected, but we also had several surprises for which we can offer no explanation and which may perhaps be worth further investigation. There can be no doubt that, for a given Liouvillian, the rate of growth of the D entropy depends on the symmetry class of the Liouville density. Therefore, contrary to the Kolmogorov-Sinai entropy [11,12], the D-entropy is not directly related to the Lyapunov exponent of classical trajectories.

Even more surprising is a quantitative comparison of Figs. 3 and 4. The growth of S for a pure twist (which is a regular mapping) is *faster* than its growth for a weakly chaotic twist and turn map (with low a), when we compare the total twist angle in the first case and the sum of discontinuous twists of the discrete map. For example, after ten steps with $a = 1.5$, we have $S = 2.018$, while, for the same initial state (19), a pure twist of 15 rad gives a larger entropy $S = 2.740$.

The initial motivation of this work was a search for the existence of genuine quantum chaos, namely, quantum wave functions whose complexity would increase exponentially with time and whose long-range evolution would therefore be uncomputable [18]. How to contruct such a quantum chaotic system (with a continuous spectrum, of course) will be discussed in a forthcoming paper [19].

ACKNOWLEDGMENTS

This work was supported by the Gerard Swope Fund and the Fund for Encouragement of Research.

APPENDIX A: THE LYAPUNOV EXPONENT

Consider infinitesimal deviations $x \to x + \epsilon\xi$, $y \to y + \epsilon\eta$, and $z \to z + \epsilon\zeta$, from a fiducial orbit of the map (6). These deviations satisfy

$$x\xi + y\eta + z\zeta = 0, \tag{A1}$$

so as to lie on the surface of the sphere. We can also define the tangential components of the vector (ξ, η, ζ), namely,

$$u = (-y\xi + x\eta)/\sqrt{1 - z^2}, \quad v = \zeta/\sqrt{1 - z^2}, \tag{A2}$$

in the "east" and "north" directions, respectively.

Likewise, at the next step, let $x' \to x' + \epsilon\xi'$, etc. Neglecting terms of order ϵ^2 and higher, we obtain, from Eq. (6),

$$\begin{aligned} \xi' &= \zeta, \\ \eta' &= \xi \sin(az) + \eta \cos(az) - \zeta a z', \\ \zeta' &= -\xi \cos(az) + \eta \sin(az) + \zeta a y'. \end{aligned} \tag{A3}$$

This set of equations is the *linear* dynamical law for the evolution of the vector (ξ, η, ζ). We now want to know how an infinitesimal "unit" circle, namely, a set of points with initial components $u = \cos\alpha$, $v = \sin\alpha$ (where α runs from 0 to 2π), transforms into an ellipse (with the same area). The asymptotic growth of the major axis of this ellipse gives the Lyapunov exponent, as defined by Eq. (7).

To find how this infinitesimal circle transforms, we note that, by virtue of the linearity of (A3), if the initial components of a tangential vector are $(\cos\alpha)$ and $(\sin\alpha)$, these components become, after a number of steps, $(T_{11}\cos\alpha + T_{12}\sin\alpha)$ and $(T_{21}\cos\alpha + T_{22}\sin\alpha)$, respectively, where the coefficients T_{pq} are independent of α. It is therefore enough to consider two infinitesimal tangent vectors having, initially, $\alpha = 0$ and $\pi/2$. Their evolution determines all the components of T_{pq} and the length of the semimajor axis is then obtained by maximizing the expression

$$r^2(\alpha) = (T_{11}\cos\alpha + T_{12}\sin\alpha)^2 + (T_{21}\cos\alpha + T_{22}\sin\alpha)^2 \tag{A4}$$

as a function of α. The result after n steps is

$$a_n = [\sigma + (\sigma^2 - 1)^{1/2}]^{1/2}, \tag{A5}$$

where $\sigma = \sum_{pq}(T_{pq})^2$. Finally, the Lyapunov exponent is given by Eq. (7), in the limit $n \to \infty$.

We must still explain the dispersion of the results shown in Fig. 2. For this, we note that there is an infinite number of *closed* (periodic) orbits having their own "private" Lyapunov exponents, which are different from the unique Lyapunov exponent of generic open chaotic orbits. For example, the point (0,1,0) is invariant under the mapping (6). This fixed point thus is by itself an orbit of period one, for which it is easy to find the eigenvalues of the linear transformation (A3). These are

$[(a/2)^2-1]^{1/2}\pm(a/2)$, giving $\lambda=0.962$, a result much larger than the one in Eq. (8). Other unstable periodic orbits also have widely different Lyapunov exponents.

There is an infinite number of these periodic orbits. They are dense in phase space, even though they are a set of measure zero among all possible orbits. Thus any generic ergodic orbit has segments that are very close to any one of these periodic orbits. In each such segment, there is a different "local" λ. As the ergodic orbit proceeds, it samples more and more vicinities of periodic orbits and in this way a definite average λ emerges. Finding λ from a single orbit therefore requires a very long one, typically 10^5 steps. In our work, we did not attempt to follow such a long orbit, which would have required special techniques [13]. Instead, we relied on the fact that a mixing system is always ergodic, so that a time average is equal to a phase space average: many evenly spread short orbits give the same average result as a very long one.

APPENDIX B: THE TWIST MATRIX

The evaluation of the matrix elements $U_{jl}^{(m)}$ in Eq. (18) is the procedure that consumes most of the time in our calculations. Each one of the indices j,l,m may run up to 500. There are therefore many millions of different integrals for which no analytic expression is known. These integrals are, for large values of their indices, rapidly varying functions of $\cos\theta$, and a straightforward numerical integration, with the level of accuracy that we wanted, would be prohibitive.

We took advantage of the fact that a twist by a finite angle a can be generated by a sequence of infinitesimal twists by an angle ϵ, for which we can replace $e^{-im\epsilon z}$ by $(1-im\epsilon z)$. This entails no loss of precision if $m\epsilon<10^{-16}$, when we compute with 16 significant digits. The matrix elements $U_{jl}^{(m)}(\epsilon)$ can be evaluated explicitly (see below) and each matrix is then raised to the appropriate power. For example, by taking $\epsilon=2^{-k}a$, we merely have to compute $(\cdots((U^2)^2)^2\cdots)^2$, k times.

We only explicitly need

$$\int Y_j^{m*}(\theta,\phi)\,Y_l^m(\theta,\phi)\,\cos\theta\,d\Omega = \text{const}\times\int_{-1}^{1}P_j^m(z)\,P_l^m(z)\,z\,dz. \quad \text{(B1)}$$

This expression is readily evaluated by using the identity

$$z\,P_j^m(z)\equiv[(j-m+1)\,P_{j+1}^m(z)+(j+m)\,P_{j-1}^m]/(2j+1) \quad \text{(B2)}$$

and the orthogonality relations for associated Legendre polynomials [20].

APPENDIX C: THE ROTATION MATRIX

There are explicit formulas for the unitary rotation matrices $R_{mn}^{(j)}$ [16, 17]. However, when j is large, these formulas are not convenient for numerical calculations because each matrix element is given as the tiny sum of a large number of huge terms with opposite signs. Only a few elements with $m=\pm j$, or m close to $\pm j$, can easily be obtained from the general formula.

A much more efficient way of obtaining the R matrix for a 90° turn around the y axis is to use its very definition, namely, $R^\dagger J_x R=J_z$, or

$$J_x\,R=R\,J_z. \quad \text{(C1)}$$

With the standard representation, namely $(J_z)_{mn}=m\delta_{mn}$ and J_x real, this gives

$$[(j+m)\,(j-m+1)]^{1/2}\,R_{m-1,n}^{(j)} +[(j+m+1)\,(j-m)]^{1/2}\,R_{m+1,n}^{(j)}=2n\,R_{mn}^{(j)}. \quad \text{(C2)}$$

Let us therefore define, for each j and n, a "vector" V_m by

$$R_{mn}^{(j)}=\frac{(-1)^{n-m}}{2^j}\left[\frac{(j+m)!\,(j-m)!}{(j+n)!\,(j-n)!}\right]^{1/2}V_m. \quad \text{(C3)}$$

From the explicit formulas mentioned above [16, 17], it can be seen that all the components of V_m are integers and in particular $V_{-j}=1$ and $V_{1-j}=2n$. The recursion relation (C2) thus becomes

$$(j-m+1)\,V_{m-1}-2n\,V_m+(j+m+1)\,V_{m+1}=0. \quad \text{(C4)}$$

(This equation also appeared as the last equation of Ref. [9], unfortunately marred by a misprint. The calculations in ref. [9] were correct.)

Even with the simple recursion formula (C4), it is not trivial to obtain all the V_m for $j>50$ (when using double precision floating point arithmetics) because the recursion is unstable and small numerical errors grow exponentially. We therefore performed this calculation *exactly*, using integer arithmetics, and we checked that the resulting matrices were indeed unitary.

APPENDIX D: BASIS INDEPENDENCE

The dimensional entropy defined by Eq. (5) obviously depends on the choice of the orthonormal basis $\{u_n\}$. We shall now present a qualitative argument (not a formal proof) that, for a reasonable choice of the basis, the asymptotic growth of S is almost independent of the basis. By "reasonable" we mean that the construction of the basis involves only a small amount of algorithmic information and in particular that it is independent of our knowledge of the evolution of ρ. Indeed, if we consider another reasonable basis $\{v_\alpha\}$, the unitary matrix with elements $\langle u_n,v_\alpha\rangle$ is a *band matrix*: only a finite number of terms appreciably contribute to the normalization of each one of the rows and columns of that matrix.

Consider now some ρ for which S, computed with the

basis $\{u_n\}$, is large. The number of non-negligible coefficients $\langle \rho, u_n \rangle$ that appreciably contribute to the expansion of ρ is about e^S and typical values of $|\langle \rho, u_n \rangle|^2$ are about e^{-S}. For another basis $\{v_\alpha\}$, we have

$$\langle \rho, v_\alpha \rangle = \sum_n \langle \rho, u_n \rangle \langle u_n, v_\alpha \rangle. \tag{D1}$$

This infinite sum effectively has only a finite number of non-negligible terms, say b, because of the finite width of the band matrix $\langle u_n, v_\alpha \rangle$. Consider now the asymptotic limit $e^S \gg b^2$. It follows from Eq. (D1) that if $|\langle \rho, u_n \rangle|^2$ is of the order of e^{-S}, the order of magnitude of $|\langle \rho, v_\alpha \rangle|^2$ is about $e^{-S \pm 2 \ln b}$. Therefore, for finite b and $S \to \infty$, the D entropies in the two bases have the same asymptotic values.

[1] B. O. Koopman, Proc. Natl. Acad. Sci. U.S.A. **17**, 315 (1931).

[2] P. R. Halmos, *Lectures on Ergodic Theory* (Chelsea, New York, 1956), pp. 34–46.

[3] V. I. Arnold and A. Avez, *Ergodic Problems of Classical Mechanics* (Benjamin, New York, 1968), p. 17.

[4] I. C. Percival, J. Math. Phys. **2**, 235 (1961).

[5] H. J. Korsch and M. V. Berry, Physica D **3**, 627 (1981).

[6] F. M. Izrailev, Phys. Lett. A **134**, 13 (1988); J. Phys. A **22**, 865 (1989).

[7] Y. V. Fyodorov and A. D. Merlin, Phys. Rev. Lett. **71**, 412 (1993).

[8] F. Haake, M. Kuś, and R. Scharf, Z. Phys. B **65**, 381 (1987).

[9] A. Peres, in *Quantum Chaos*, Proceedings of the Adriatico Research Conference on Quantum Chaos, edited by H. A. Cerdeira, R. Ramaswamy, M. C. Gutzwiller, and G. Casati (World Scientific, Singapore, 1991), pp. 73–102.

[10] A. Peres, *Quantum Theory: Concepts and Methods* (Kluwer, Dordrecht, 1993), pp. 354–358.

[11] L. E. Reichl, *The Transition to Chaos* (Springer, New York, 1992), pp. 46–51.

[12] M. Tabor, *Chaos and Integrability in Nonlinear Dynamics* (Wiley, New York, 1989), pp. 148–151.

[13] S. Habib and R. D. Ryne, Phys. Rev. Lett. **74**, 70 (1995).

[14] S. Gasiorowicz, *Quantum Physics* (Wiley, New York, 1974), p. 175.

[15] E. Merzbacher, *Quantum Mechanics* (Wiley, New York, 1970), p. 185.

[16] E. P. Wigner, *Group Theory and Its Application to the Quantum Mechanics of Atomic Spectra* (Academic, New York, 1959), p. 167.

[17] M. Tinkham, *Group Theory and Quantum Mechanics* (McGraw-Hill, New York, 1964), p. 110.

[18] J. Ford, in *Chaotic Dynamics and Fractals*, edited by M. F. Barnsley and S. G. Demko (Academic, New York, 1986), pp. 1–52.

[19] A. Peres (unpublished).

[20] *Handbook of Mathematical Functions*, edited by M. Abramowitz and I. A. Stegun (Dover, New York, 1972), p. 334.